Second Harmonic Generation of Unpolarized Light

Changqin Ding, James R. W. Ulcickas, Fengyuan Deng, and Garth J. Simpson

Department of Chemistry, Purdue University, 560 Oval Drive, West Lafayette, Indiana 47907, USA

A Mueller tensor mathematical framework was applied for predicting and interpreting the second harmonic generation (SHG) produced with an unpolarized fundamental beam. In deep tissue imaging through SHG and multiphoton fluorescence, partial or complete depolarization of the incident light complicates polarization analysis. The proposed framework has the distinct advantage of seamlessly merging the purely polarized theory based on the Jones or Cartesian susceptibility tensors with a more general Mueller tensor framework capable of handling partial depolarized fundamental and/or SHG produced. The predictions of the model are in excellent agreement with experimental measurements of z-cut quartz and mouse tail tendon obtained with polarized and depolarized incident light. The polarization-dependent SHG produced with unpolarized fundamental allowed determination of collagen fiber orientation in agreement with orthogonal methods based on image analysis. This method has the distinct advantage of being immune to birefringence or depolarization of the fundamental beam for structural analysis of tissues.

Second harmonic generation (SHG) is a second order nonlinear optical (NLO) process allowed for structures without an inversion center. The polarization dependence of SHG provides rich information on orientation and arrangement of local structures, as demonstrated for characterization of biostructures [1–4], protein crystals [5], and active pharmaceutical ingredients [5,6]. However, structural information is routinely lost in measurements designed to take advantage of the increased penetration depth of nonlinear optical interactions. In beam-scanning instruments, image contrast in SHG is generally retained in turbid media for much greater depths than analogous linear interactions [7–9]. However, the native turbidity and/or birefringence of biological media have the potential to complicate polarization dependent measurements through partial or complete depolarization of the incident and/or detected light.

Several studies have considered the effects of partial depolarization in polarization-dependent NLO imaging via the cumulative effects of scattering, birefringence, and linear or circular dichroism [3,4,10]. Optical clearing mitigates the effects of scattering by refractive index matching [11]. Careful bookkeeping of polarization-state changes has been used to remove bias in recovered tensor elements from polarization resolved SHG microscopy at tissue depths of 100 μm [3,4,10]. However, such methods do not account for the influence of depolarization arising from heterogeneity within the sample during propagation to the object plane. More recently, Mueller tensor methods have been introduced for quantitatively understanding and correcting for depolarization effects in nonlinear optical measurements. Barzda and co-workers have introduced the Stokes-Mueller framework for the theoretical description of nonlinear optical polarimetry based on a "super-Mueller

matrix" approach originally developed by Mclain and Shi [12–14]. This approach has been used to study crystalline and collagen fibril organization for polarization dependent measurements [15,16]. However, a large number of observables with many different incident polarization states are required in order to populate all 36 unique elements of the super-Mueller matrix. In a recent complementary framework [17], the Mueller tensors in partially depolarizing assemblies were greatly simplified by directly bridging Jones and Mueller tensors. The role of partial depolarization can in principle be incorporated by a single additional adjustable parameter relative to analogous measurements in nondepolarizing assemblies.

In principle, linear optical interactions can be used to describe much of the depolarization effects in nonlinear optics. In SHG microscopy of turbid media, the collective process can be conceptually broken down into three key steps: (i) propagation of the fundamental beam through the turbid matrix to the object plane, (ii) production of SHG by the object of interest by the Mueller tensor $M^{(2)}$, and (iii) propagation of the frequency-doubled light to the far-field detector. In steps (i) and (iii), partial depolarization of the incident and detected beams can, in principal, be handled by conventional linear Mueller matrices. Step (ii) cannot be described by either linear Mueller matrix transformations or considerations of conventional nonlinear polarizability based on Jones and/or Cartesian tensors.

In this Letter, the process of SHG driven by unpolarized light was considered both theoretically and experimentally, then applied to recover both polar and azimuthal orientation of collagen fibrils. In a model system, predictions from a mathematical framework connecting Jones and Mueller tensors [17] were compared with observations for z-cut

quartz. With this framework in place, polarization-dependent SHG from partial or complete depolarization of the incident beam can be quantitatively described using the intuitive Jones tensor.

In the simplest model for partial depolarization, the fundamental light reaching the object plane is considered as a linear combination of a purely depolarized fraction and a residual purely polarized component. The purely polarized fundamental surviving to the focal plane can be related to the corresponding purely polarized SHG produced locally $(\vec{e}^{2\omega})$ by a Jones tensor formalism. The Jones vector can be connected to the more general Stokes vector with a transformation matrix A, such that $\vec{s}^{2\omega} = A \cdot (\vec{e}^{2\omega} \otimes \vec{e}^{2\omega})$.

In linear optics, connecting the Mueller matrices to Jones matrices provides an intuitive framework for interpreting polarization propagation. Using the preceding relationship allows the 4×4 Mueller matrix M to be written in terms of the 2×2 Jones matrix J: $M = A \cdot (J \otimes J) \cdot A^{-1}$.

In the theoretical framework developed previously [17], these connections between Mueller and Jones matrices in linear optics were shown to be directly extendable to nonlinear optics, in which the elements of the $4 \times 4 \times 4$ Mueller tensor describing SHG $M^{(2)}$ driven by partially or fully depolarized incident light are connected back to combinations of simpler $2 \times 2 \times 2$ Jones tensor elements $\chi_J^{(2)}$ using the matrix A [Eq. (1) and Supplemental Material, Eqs. (S6)–(S9) [18]] [17,19].

$$M^{(2)} = A \cdot (\chi_J^{(2)*} \otimes \chi_J^{(2)}) : A^{-1}A^{-1}. \tag{1}$$

The detected Stokes vector depends on 16 products of Jones tensor elements, which are combinations of Jones tensor elements contributing to the SHG produced with unpolarized incident light. The Stokes vector for the fraction of SHG produced from a fully depolarized beam maps onto four Mueller tensor elements: M_{000}, M_{110}, M_{200}, and M_{300} [Supplemental Material Eqs. (S1)–(S5) [18]]. As shown in Eq. (2), the nonzero Jones tensor elements can be written in four groups, with the first index in each of the χ_{ijk} tensor elements corresponding to the electric field component produced by the nonlinear optical process [Supplemental Material, Eqs. (S10-S14) [18]]. Zero indicates the laboratory horizontal axis and 1 indicates the laboratory vertical axis (Sec. II. 2 of the Supplemental Material [18]).

$$\begin{bmatrix} s_0 \\ s_1 \\ s_2 \\ s_3 \end{bmatrix}^{2\omega} = \frac{1}{4} \begin{bmatrix} 1 & 0 & 0 & 1 \\ 1 & 0 & 0 & -1 \\ 0 & 1 & 1 & 0 \\ 0 & i & -i & 0 \end{bmatrix}$$

$$\cdot \begin{bmatrix} \chi_{000}^*\chi_{000} + \chi_{001}^*\chi_{001} + \chi_{010}^*\chi_{010} + \chi_{011}^*\chi_{011} \\ \chi_{000}^*\chi_{100} + \chi_{001}^*\chi_{101} + \chi_{010}^*\chi_{110} + \chi_{011}^*\chi_{111} \\ \chi_{100}^*\chi_{000} + \chi_{101}^*\chi_{001} + \chi_{110}^*\chi_{010} + \chi_{111}^*\chi_{011} \\ \chi_{100}^*\chi_{100} + \chi_{101}^*\chi_{101} + \chi_{110}^*\chi_{110} + \chi_{111}^*\chi_{111} \end{bmatrix}. \tag{2}$$

The nonzero Jones tensor elements can be further reduced by considering the symmetry within the local-frame systems. For the specific case of collagen (or any uniaxial assembly), the nonzero elements within the local frame are $\chi_{z'z'z'}$, $\chi_{z'x'x'} = \chi_{z'y'y'}$, $\chi_{x'x'z'} = \chi_{x'z'x'}$ and $\chi_{x'y'z'} = \chi_{x'z'y'} = -\chi_{y'x'z'} = -\chi_{y'z'x'}$, with the z' axis defined as the unique fiber axis. From quantum chemical calculations, the chiral terms are predicted to be relatively weak in collagen performed far from resonance, and disappear by symmetry for fibers aligned within the field of view (FOV) [4,20].

The Jones-Mueller connection enables quantitative prediction of the SHG produced from depolarized light using the knowledge of SHG originating for pure polarization states. If it is initially assumed for illustrative purposes that the local-frame z' axis of the collagen fiber axis is oriented coparallel with the laboratory Jones frame horizontal (0) axis and the x' axis is coparallel with the laboratory vertical (1) axis, the following nonzero elements remain in the laboratory-frame Jones tensor: $\chi_{000} = \chi_{z'z'z'}$, $\chi_{011} = \chi_{z'x'x'}$, and $\chi_{110} = \chi_{101} = \chi_{x'x'z'}$. For purely polarized incident light, the z'-polarized SHG is given by the coherent combination of contributions from χ_{000} and χ_{011}, the relative magnitudes and phases of which depend on the incident polarization state. Similarly, the x'-polarized component scales with the χ_{101} driven by the component of the incident light with both x' and z' polarizations.

For unpolarized incident light, the SHG can be considered as arising from the incoherent summation of these three contributions [given by the corresponding entries in the rightmost matrix in Eq. (2)]. Introduction of rotation matrices enables analysis of fibers oriented an arbitrary azimuthal angle (ϕ). Equation (2) can be rewritten as Eq. (3), which is a simplified form of Eq. (S14). The rotation operations can be applied to either the Mueller tensor as shown in Eq. (3) or to the Kronecker product of Jones tensors (detailed in Supplemental Material [18]).

$$\begin{bmatrix} s_0 \\ s_1 \\ s_2 \\ s_3 \end{bmatrix}^{2\omega} = \frac{1}{4} \begin{bmatrix} 1 & 1 & 1 \\ \cos(2\phi) & \cos(2\phi) & -\cos(2\phi) \\ -\sin(2\phi) & -\sin(2\phi) & \sin(2\phi) \\ 0 & 0 & 0 \end{bmatrix} \begin{bmatrix} |\chi_{z'z'z'}|^2 \\ |\chi_{z'x'x'}|^2 \\ 2|\chi_{x'x'z'}|^2 \end{bmatrix}. \tag{3}$$

Consistent with previous reports [3–5,15] for z-cut quartz and collagen far from resonance, Eq. (3) can be simplified by making the approximation of $|\chi_{z'x'x'}| \cong |\chi_{x'x'z'}|$ and rewritten with two parameters: the azimuthal rotation angle ϕ and a defined ratio $\rho \equiv \chi_{z'z'z'}/\chi_{z'x'x'}$.
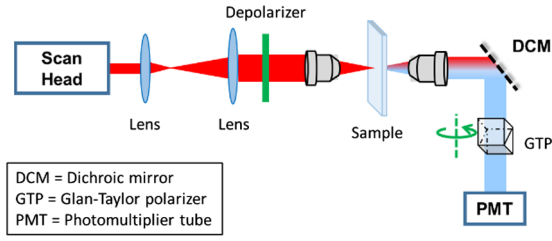
FIG. 1. SHG transmittance microscope capable of delivering both a purely polarized and a depolarized fundamental beam.

$$\begin{bmatrix} s_0 \\ s_1 \\ s_2 \\ s_3 \end{bmatrix}^{2\omega} = \frac{|\chi_{z'x'x'}|^2}{4} \begin{bmatrix} 1 & 1 & 1 \\ \cos(2\phi) & \cos(2\phi) & -\cos(2\phi) \\ -\sin(2\phi) & -\sin(2\phi) & \sin(2\phi) \\ 0 & 0 & 0 \end{bmatrix} \begin{bmatrix} |\rho|^2 \\ 1 \\ 2 \end{bmatrix}. \tag{4}$$

While Eqs. (3) and (4) are derived under the assumption that the sample is aligned within the FOV with polar tilt angle of $\pi/2$ and ρ equal to the local frame ratio given above, the same tensor elements are also present for collagen with tilt angles other than $\pi/2$ (neglecting relatively weak chiral-specific contributions). In those cases, ρ equals to the ratio of projected $\chi_{z'z'z'}$ and $\chi_{z'x'x'}$ within the FoV, defined as χ_{XXX}/χ_{XYY} (detailed in Supplemental Material [18]). To avoid confusion in the later discussion, ρ_l is defined as the local frame tensor ratio with tilt angle $\theta = \pi/2$, and ρ as the measured laboratory-frame ratio χ_{XXX}/χ_{XYY} for any arbitrary tilt angle θ.

The detected SHG intensity after a postsample polarizer at angle ϕ_{pol} can be calculated based on the Stokes vector, with s_0 normalized to unity through the proportionality constant C,

$$I^{2\omega}(\phi_{\mathrm{pol}}) = \frac{C}{2}[s_0 + s_1 \cos(2\phi_{\mathrm{pol}}) - s_2 \sin(2\phi_{\mathrm{pol}})]. \tag{5}$$

Combining Eqs. (4) and (5), the measured laboratory-frame ratio ρ can be determined by a linear fit to the measured intensities based on Eq. (6).

$$I^{2\omega}(\phi_{\mathrm{pol}}) = \frac{C}{8}[(|\rho|^2 + 3) + (|\rho|^2 - 1)\cos(2\phi_{\mathrm{pol}} - 2\phi)]. \tag{6}$$

To evaluate this theory, SHG measurements were performed with a custom-built microscope described in detail previously [5]. For measurements of SHG generated from a depolarized incident beam, a depolarizer (DPP-25B, Thorlabs) was placed in the collimated path (Fig. 1). A Glan-Taylor polarizer was inserted in a rotation stage in front of the detector. SHG intensity was recorded following mechanical rotation of the polarizer from 0 to π rad (ϕ_{pol})

with 60 intervals illuminated with both a purely polarized and a depolarized incident beam.

SHG produced from z-cut quartz was measured to assess the predictions for a model system with well-established nonlinear optical properties exhibiting no birefringence for light propagating parallel to the z axis. Polarized SHG produced by z-cut quartz from purely vertically polarized incident light was shown in Fig. 2. The SHG intensities integrated over the whole FOV was fit to Eq. (7) (detailed in the Supplemental Material [18] with Ref. [21]), relating to the detected polarization angle [ϕ_{pol}, Fig. 2(a)] or the quartz orientation angle [azimuthal angle ϕ, Fig. 2(b)]. Good agreement between the fitted curve (green lines) and experiment SHG intensity (blue markers) was observed, with the threefold higher periodicity in azimuthal angle in Fig. 2(b) is a consequence of the threefold rotational symmetry of z-cut quartz,

$$I^{2\omega}(\phi, \phi_{\mathrm{pol}}) = C\sin^2(3\phi - \phi_{\mathrm{pol}}). \tag{7}$$

For SHG produced by z-cut quartz for a depolarized incident beam, the ratio $\rho = -1$ by symmetry, such that Eq. (5) predicts the production of SHG intensity that is completely independent of both the polarizer rotation angle ϕ_{pol} and quartz orientation angle ϕ. This outcome is consistent with the production of entirely unpolarized SHG from z-cut quartz, with intensity equal to half the amplitude observed from the purely polarized source. The theoretical result is shown in purple lines in Fig. 2, together with the experimental observations (red dots) as ϕ_{pol} is varied. The predications are in excellent agreement with the theoretical prediction. It is worth emphasizing that the theoretical trace is not a fit to the unpolarized data, but rather the predicted behavior with no adjustable parameters based on the observed trends for a polarized source. Analogous measurements performed as a function of ϕ
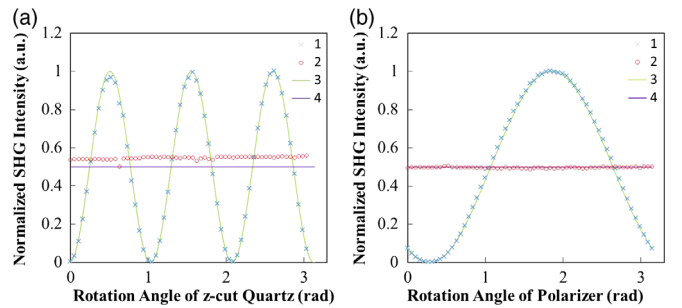

FIG. 2. (a) Polarization dependent measurement of SHG signal from z-cut quartz at an arbitrary angle under (1) vertically polarized and (2) depolarized incident light overlay with theoretical (3) fitting and (4) prediction. (b) Measurements of horizontally polarization SHG signals from z-cut quartz at different azimuthal angle under (1) vertically polarized and (2) depolarized incident light, with theoretical (3) fitting and (4) prediction.

with a fixed detector polarization rotation angle ϕ_{pol} and z-cut quartz rotation showed similar agreement between theory and experiments [Fig. 2(b)]. Although the depolarized result yields a slight offset from predictions based on the polarized measurements, the overall independence of the SHG measured through a fixed polarizer as a function of the quartz rotation angle was consistent with the expectations from the theoretical predictions. The observed offset was tentatively attributed to uncertainty in the amplitude determined from the fits of the traces observed with a purely polarized input. The excellent overall agreement between theory and experiment generally supports the validity of the mathematical framework and its approximations for describing the coherent process of SHG driven by partially or wholly depolarized light.

SHG produced from collagen within a longitudinally sectioned mouse tail was also analyzed with depolarized incident light. The local fiber orientations (ϕ) and tensor ratios (ρ) were then retrieved for every SHG-active pixel by fitting the intensity trend as a function of ϕ_{pol} described in Eq. (6). From the per-pixel fitting, the azimuthal angle of collagen was determined at a per-pixel basis for each location exhibiting sufficient signal to noise to allow statistically significant polarization analysis [Fig. 3(a)]. Unlike the case for z-cut quartz, the polarization-dependent SHG produced from a depolarized fundamental beam generally exhibited SHG with strong polarization preferences, consistent with Eq. (6) for $|\rho| \neq 1$. A representative fit is shown in Fig. 3(d).

The local azimuthal orientations of the collagen fibers were also independently determined by ORIENTATIONJ, a plugin for image directional analysis for IMAGEJ [22,23]. Figure 3(a) demonstrates the intensity-weighted orientation map retrieved via pixel-by-pixel nonlinear fit, contrasted with the orientation map recovered by ORIENTATIONJ in Fig. 3(b). Good agreement between the two methods was observed for local azimuthal orientations. Figure 3(c) shows an overlay of histogram of orientation angles recovered via both methods. Notably, ORIENTATIONJ assigns orientation based entirely on image analysis relying on context from adjacent pixels. As such, the two methods for determining azimuthal orientation (single pixel polarization analysis and contextual image analysis) are orthogonal methods yielding comparable outcomes.

Several possible explanations may account for the subtle but nonzero deviations between fiber orientation angles determined by polarization analysis versus image analysis (ORIENTATIONJ). First, the depolarizer functions by imposing a sinusoidal modulation of the polarization state across the physical expanse of the collimated beam. Upon passing this beam through the objective, the spatial Fourier transform of a sinusoidal modulation results in a horizontally offset dual-spot point spread function within the FOV, which in turn produces a double image. The SHG produced from a depolarized source should contain equal
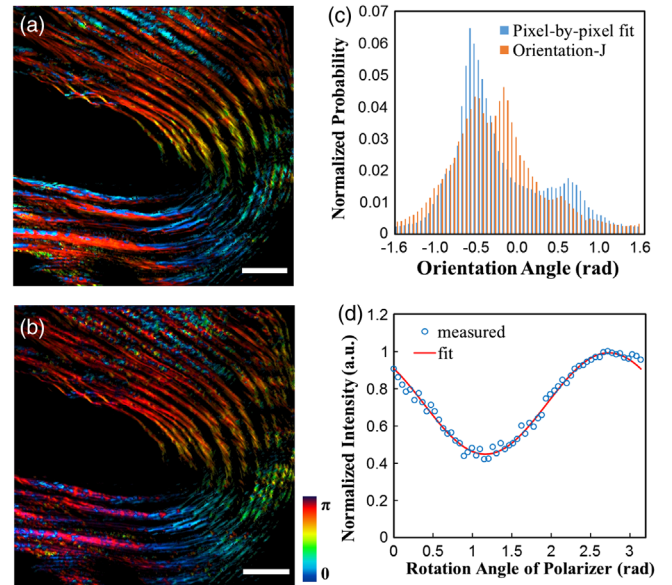

FIG. 3. Orientation images of the azimuthal angle for a single FOV of mouse tail section from (a) the pixel-by-pixel nonlinear fit analysis and (b) ORIENTATIONJ. Scale bar: 100 μm. (c) The histogram of the orientation distribution achieved from pixel-by-pixel fit and ORIENTATIONJ. (d) Nonlinear fitting results of depolarized light excitation SHG for signal random pixel.

contributions from both foci in order to be considered as genuinely depolarized. Spatial variation across the FOV may significantly influence the validity of this assumption, given that the fiber thickness is generally small relative to the displacement. Polarization analysis performed for both vertically and horizontally aligned collagen regions were compared to assess the potential impact of the double beam in polarization analysis. Given that the offset is solely along the horizontal axis, perturbations from the double focus should be significantly more pronounced for vertically oriented fibers. From inspection of the images, comparable deviations were observed for both horizontally and vertically aligned fibers, suggesting the absence of obvious systematic bias from the particular manner in which the beam was rendered unpolarized in the present study.

In addition to recovering the azimuthal angle, the polarization-dependent SHG generated from an unpolarized source also allows recovery of the measured laboratory-frame ratio ρ through Eq. (6), with representative images shown in Fig. 4(a). The modal value of $\rho = 1.69$ [Fig. 4(c)] is consistent with several other previous reports [4,24] for mouse tail and other collagenous assemblies such as chicken wing and human dermis. Deviations between polarization analysis and image analysis may arise from the implicit assumption that the fibers exhibit polar tilt angles of $\pi/2$, such that the fibers are assumed to lie flat within the FOV. In practice, any thin section is generally expected to transect a given fiber at a nozero polar angle θ. Whereas image analysis methods such as ORIENTATIONJ can independently inform azimuthal orientation, polar tilt remains a
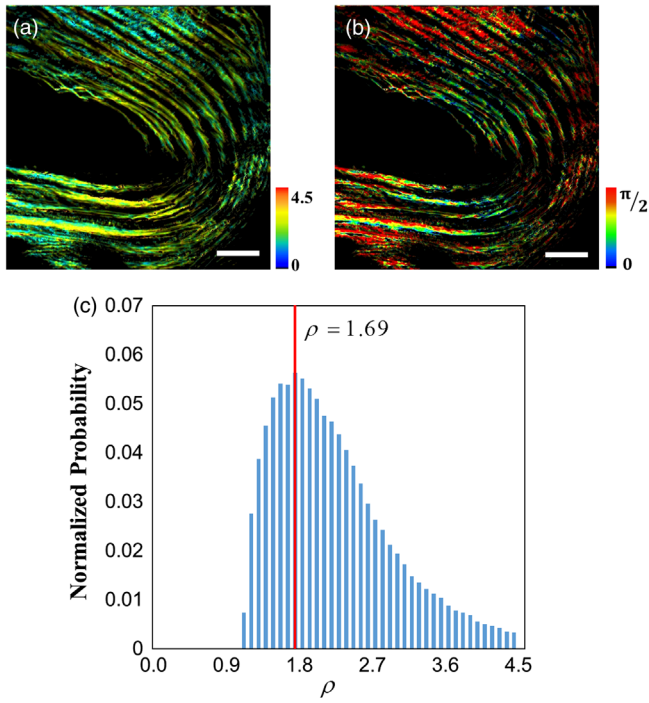
FIG. 4. (a) The measured laboratory-frame ratio ρ images for a single FOV of mouse tail section from the per-pixel fit analysis. (b) The polar tilt angle θ image recovered from the measured laboratory-frame ratio ρ for the same FOV with $\rho_l = 1.7$. (c) The distribution of the ratio ρ, with the maximum peak marked at 1.69. Scale bar: 100 μm.

challenge. Fortunately, the polarization-dependent SHG may provide a route for accessing polar tilt angle, provided the value of ρ can be independently measured or assumed.

Using literature values for the local-frame ratio ρ_l (i.e., relative to the long axis of an individual collagen fiber), a mathematical relation between measured laboratory-frame ratio (ρ), the local-frame ratio ρ_l, and the polar tilt angle (θ) was derived in Eq. (8) by projecting local tensor element onto the lab frame [25] (detailed in the Supplemental Material [18]),

$$\theta = \arcsin\left(\sqrt{\frac{\rho - 3}{\rho_l - 3}}\right). \qquad (8)$$

A per-pixel fit was performed to recover a map of polar tilt angle θ with the assumption of a local-frame hyperpolarizability ratio $\rho_l = 1.7$ based on previously reported values in which the range of the polar tilt angle at each pixel was determined experimentally [4,15]. This value of the local-frame ratio for collagen fibers is quite similar to the most probable ratio observed experimentally [Fig. 4(c)], consistent with an assembly in which the most probable collagen orientation is lying flat within the field of view. With the assumption of $\rho_l = 1.7$, the observed values of ρ were used to recover the polar tilt angle at each pixel through Eq. (8). The recovered map of polar tilt angle θ was

shown in Fig. 4(b). A significant portion of collagen fibers was tilted out of the detection plane (i.e., $\theta \neq \pi/2$). This phenomenon was more obvious in the region where collagen fibers bend. The measurements likely contain an implicit bias against tilt angles of $\theta \cong 0$, as fibers aligned parallel with the optical access are symmetry forbidden for production of coherent SHG. The results shown in Fig. 4 are largely insensitive to the particular assumed value of ρ_l, yielding qualitatively similar results when assuming $\rho_l = 1.4$ (consistent with other reports for the local-frame tensor element ratio) [4,15].

In summary, the results of this study have intriguing implications on polarization analysis of depolarizing systems. A Mueller tensor framework was utilized to predict the polarization of SHG stimulated with depolarized light. This framework has been verified experimentally with z-cut quartz and collagenous tissue under depolarized incident light. From a practical standpoint, the intentional use of depolarized incident light has the distinct advantage of providing measurements that are immune to subsequent depolarization of the fundamental beam. Despite the loss of information from scrambling of the incident polarization, analysis of collagenous tissue with depolarized SHG still allowed determination of both collagen azimuthal and polar orientation from the laboratory-frame tensor elements. The use of unpolarized incident light may significantly simplify polarization analysis in thick tissue sections for measurement in transmission.

[1] P. J. Campagnola and L. M. Loew, Nat. Biotechnol. **21**, 1356 (2003).
[2] P. Stoller, K. M. Reiser, P. M. Celliers, and A. M. Rubenchik, Biophys. J. **82**, 3330 (2002).
[3] I. Gusachenko, V. Tran, Y. Goulam Houssen, J. M. Allain, and M. C. Schanne-Klein, Biophys. J. **102**, 2220 (2012).
[4] X. Y. Dow, E. L. DeWalt, S. Z. Sullivan, P. D. Schmitt, J. R. Ulcickas, and G. J. Simpson, Biophys. J. **111**, 1361 (2016).
[5] E. L. DeWalt, S. Z. Sullivan, P. D. Schmitt, R. D. Muir, and G. J. Simpson, Anal. Chem. **86**, 8448 (2014).
[6] P. D. Schmitt, E. L. DeWalt, X. Y. Dow, and G. J. Simpson, Anal. Chem. **88**, 5760 (2016).
[7] T. Petralli-Mallow, T. M. Wong, J. D. Byers, and H. I. Yee, J. Phys. Chem. **97**, 1383 (1993).
[8] F. Tiaho, G. Recher, and D. Rouede, Opt. Express **15**, 12286 (2007).
[9] I. Amat-Roldan, S. Psilodimitrakopoulos, P. Loza-Alvarez, and D. Artigas, Opt. Express **18**, 17209 (2010).
[10] I. Gusachenko, G. Latour, and M. C. Schanne-Klein, Opt. Express **18**, 19339 (2010).
[11] O. Nadiarnykh and P. J. Campagnola, Opt. Express **17**, 5794 (2009).

[12] M. Samim, S. Krouglov, and V. Barzda, Phys. Rev. A **93,** 013847 (2016).

[13] Y. M. Shi, W. M. Mcclain, and R. A. Harris, Chem. Phys. Lett. **205,** 91 (1993).

[14] Y. M. Shi, W. M. Mcclain, and R. A. Harris, Phys. Rev. A **49,** 1999 (1994).

[15] M. Burke, A. Golaraei, A. Atkins, M. Akens, V. Barzda, and C. Whyne, J. Struct. Biol. **199,** 153 (2017).

[16] R. Cisek, D. Tokarz, M. Steup, I. J. Tetlow, M. J. Emes, K. H. Hebelstrup, A. Blennow, and V. Barzda, Biomed. Opt. Express **6,** 3694 (2015).

[17] G. J. Simpson, J. Phys. Chem. B **120,** 3281 (2016).

[18] See Supplemental Material at http://link.aps.org/supplemental/10.1103/PhysRevLett.119.193901 for detailed mathematical derivation.

[19] R. M. A. Azzam and N. M. Bashara, *Ellipsometry and Polarized Light* (Elsevier, Amsterdam, 1987).

[20] M. de Wergifosse, J. de Ruyck, and B. Champagne, J. Phys. Chem. C **118,** 8595 (2014).

[21] X. Y. Dow, E. L. DeWalt, J. A. Newman, C. M. Dettmar, and G. J. Simpson, Biophys. J. **111,** 1553 (2016).

[22] C. A. Schneider, W. S. Rasband, and K. W. Eliceiri, Nat. Methods **9,** 671 (2012).

[23] Z. Puspoki, M. Storath, D. Sage, and M. Unser, Adv Anat, Embryol Cell Biol **219,** 69 (2016).

[24] W. Chen, T. Li, P. Su, C. Chou, P. T. Fwu, S. Lin, D. Kim, P. T. C. So, and C. Dong, Appl. Phys. Lett. **94,** 183902 (2009).

[25] A. J. Moad and G. J. Simpson, J. Phys. Chem. B **108,** 3548 (2004).